Electronic structure of amorphous SiO_x:H alloy films studied by x-ray emission spectroscopy: Si K, Si L, and O K emission bands

G. Wiech and H.-O. Feldhütter
Sektion Physik der Ludwig-Maximilians-Universität München, Geschwister-Scholl-Platz 1, 8000 München 22, Federal Republic of Germany

A. Šimůnek
Institute of Physics, Czech Academy of Sciences, Cukrovarnická 10, 162 00 Prague, Czech Republic
(Received 7 January 1992; revised manuscript received 5 October 1992)

We present x-ray Si K, Si L, and O K emission bands of hydrogenated amorphous SiO_x alloy films covering the concentration range $0 \le x \le 2.2$. All spectral features in the emission bands were identified and attributed to Si $3s$, Si $3p$, and O $2s$, $2p$ derived states. With increasing x, the shape and the energy position of the main features of the Si K and Si L emission bands change significantly, particularly in the concentration interval $0.5 < x < 1.5$. A comparison with available ultraviolet (UPS) and x-ray (XPS) photoemission spectra demonstrates that x-ray emission bands for a-SiO_x are more sensitive to sample composition than UPS and/or XPS spectra. The random-bonding model and the random-mixture model of the structure of SiO_x alloys are discussed in view of the x-ray emission spectra. For $x \approx 2$, the Si K, Si L, and O K spectra are very similar to those observed for α-quartz (c-SiO_2). This justifies interpretation of all features of a-SiO_2:H on the basis of c-SiO_2. We therefore performed self-consistent pseudopotential calculations of the total density of states and the local partial density of states of Si $3s$, Si $3p$, Si $3d$, O $2s$, and O $2p$ of α-quartz. The calculations confirm that due to the high electronegativity of oxygen nonbonding, Si $3d$-like states are created which, for high values of x, clearly show up in the Si L emission bands. Finally, we discuss the long-standing so-called d-orbital controversy about SiO_2 and give an explanation of it.

I. INTRODUCTION

During the past few years the amorphous system a-SiO_x has attracted a great deal of attention not only due to its applications in silicon-based industry but also because this system can be studied in a wide range of concentrations x evolving from semiconducting amorphous silicon ($x=0$) to insulating a-SiO_2. Moreover, the Si-O bond combines strong ionic and covalent bonding, and the understanding of the microscopic atomic structures and the electronic properties of this system is a challenging task in condensed-matter physics. The lack of periodicity and the disordered composition of a-SiO_x make theoretical studies difficult.[1-3] However, crystalline silicon dioxide (c-SiO_2) existing in many forms, e.g., quartz, cristobalite, tridymite, coesite, and stishovite is not easy to describe theoretically[4] and *ab initio* quantum-mechanical calculations of the structural and electronic properties of c-SiO_2 were published just recently.[5-8]

Experimentally the electronic structure of a-SiO_x alloy films with x varying in a wide range of concentrations ($0 \le x \le 2.2$) has been studied by applying photoelectron spectroscopy[9] (PES) and x-ray emission spectroscopy (XES).[10,11] Bell and Ley[9] measured the energy position of silicon and oxygen core levels and the valence-band spectra of unhydrogenated samples of SiO_x in the ultraviolet (UPS) and x-ray (XPS) photoemission spectra regimes. In our previous work[10,11] we used XES and measured the Si K and Si L emission bands of hydrogenated a-SiO_x for only a few concentrations x. We have observed a remarkable development of features in both Si K and Si L emission bands, while UPS and/or XPS valence-band spectra[9] preserve their basic structure and position of peaks throughout the concentration range.

The relative insensitivity of photoelectron valence-band spectra can be understood as a consequence of the vastly different cross sections σ of silicon and oxygen atoms[12] having the following mutual relations: UPS ($h\nu = 40.8$ eV):

$$\sigma(\text{O } 2p) \gg \sigma(\text{Si } 3s) \gtrsim \sigma(\text{Si } 3p) ,$$

$$\sigma(\text{O } 2p) \gg \sigma(\text{O } 2s) .$$

XPS ($h\nu = 1486.6$ eV):

$$\sigma(\text{Si } 3s) \gg \sigma(\text{O } 2p) \gtrsim \sigma(\text{Si } 3p) ,$$

$$\sigma(\text{O } 2s) \gg \sigma(\text{O } 2p) ,$$

$$\sigma(\text{O } 2s) \gtrsim \sigma(\text{Si } 3s) .$$

In both UPS and XPS features arising from Si $3p$-like electrons are almost suppressed. This effect is enhanced by charge transfer which additionally reduces the amount of electrons on the silicon sites due to the high electronegativity of oxygen. As a consequence the Si $3p$-like electrons which are crucial for the Si-O bonds contribute to UPS and/or XPS spectra only with very small intensities.

In this paper we present Si K, Si L, and O K emission

bands of a-SiO_x:H alloy films with x varying in small steps and covering the concentration range from $x=0$ to $x=2.2$. The Si K emission bands reflect the local silicon p-like character, the Si L emission bands the local silicon s- and d-like character, and the O K emission bands the local oxygen p-like character of the valence electrons. The presented spectra therefore provide information about the development and the behavior of all local s-, p-, and d-like symmetries of valence electrons creating Si-O bonds and originating from atomic Si $3s$, Si $3p$, and O $2p$ electrons. The main purpose of our x-ray spectroscopic study is to delineate the behavior of oxygen and silicon s-, p-, and d-like electrons, which is difficult to study by UPS and XPS measurements. Furthermore, it was our aim to elucidate the role of Si d-like electrons in the bond. Their existence has been doubted for many years and the discussion is known as the "d-orbital controversy."[13]

The paper is organized as follows. In Sec. II experimental details are given. In Sec. III the experimental results are presented and described. The discussion and interpretation of the x-ray spectra together with available photoelectron spectra is given in Sec. IV. Finally, in Sec. V all results are briefly summarized.

II. EXPERIMENT

A. Sample preparation

Details of sample preparation and sample characteristics have been published recently.[10,14] The most relevant facts will be summarized in the following.

The specimens of a-SiO_x:H were prepared by rf glow discharge of SiH_4-CO_2-H_2 gas mixtures in a capacitive reactor system. Films with low oxygen concentration ($x<0.5$) were deposited at various CO_2/SiH_4 flow rates using a rf power density of 26 mW/cm^2, while films with higher oxygen concentration were prepared at varying rf power densities (from 26 to 330 mW/cm^2). In all cases the pressure was 133 Pa, and the substrate temperature was 250 °C. The substrates were thin copper plates (25×25 mm^2).

Film thicknesses were determined with an electromechanical stylus instrument and varied between ~1 and 1.5 μm. Sample composition was determined by electron-probe analysis (with c-Si and c-SiO_2 as standards) and from IR absorption in the 980 cm^{-1} band. The content of hydrogen was estimated from IR absorption to be 10±3 at.% in a-Si:H. According to the preparation process incorporation of carbon into samples cannot be excluded. XPS and Fourier-transformed IR (FTIR) spectra, however, did not show any indication of incorporated carbon atoms, i.e., the carbon content in the samples was less than 0.5%.[14]

B. Measurement of XES spectra

The Si K, Si L, and O K emission bands were recorded employing three different spectrometers.

1. Si K emission bands

The Si K emission bands were measured with a high vacuum Johann spectrometer. The pressure in the spectrometer and the x-ray tube was below 1×10^{-5} mbar. The x-ray tube was operated at 2 kW (10 kV, 200 mA). The characteristic radiation and the bremsstrahlung of a tungsten anode were used for excitation (fluorescence excitation). The samples were separated from the anode by a 0.5-μm-thick Al foil to protect them from bombardment with ions or scattered electrons and from evaporation with tungsten of the filament. The specimens were put in the spectrometer through a lock and fixed to the water-cooled holder without breaking the vacuum.

The dispersing element was a quartz crystal ($50\times25\times0.3$ mm^3) cut parallel to the $10\bar{1}0$ plane and bent to a radius of 109 cm. The crystal holder was heated to 29 °C to keep the crystal at constant temperature. The Bragg angle for the maximum of the K emission band of c-Si (1836.0 eV) was 52.6°.

The detector was a position-sensitive flow proportional counter with a backgammon cathode operated at about 1200 V. The gas pressure (argon-methane) was about 1 atm. Details of the detector have been published elsewhere.[15] The acquisition time was up to 42 h for about 20 000 counts, depending on sample composition. The measured spectra were corrected for the sensitivity of the detector, and then a linear background was subtracted. The energy resolution of the spectrometer was about 0.8 eV.

2. Si L emission bands

The Si L emission bands were measured with a 2-m grazing incidence concave grating spectrometer using electron bombardment for excitation (3 kV, ≤0.5 mA). The pressure in the sample chamber was $1-5\times10^{-8}$ mbar, and in the spectrometer tank, 5×10^{-6} mbar. Turbomolecular and ion getter pumps were used. Therefore the vacuum was free of hydrocarbons which could have contaminated the sample surfaces.

The gold-coated blazed grating (blaze angle 3°31′; angle of incidence 86°) had 600 lines/mm. The energy resolution of the spectrometer was ~0.7 eV at 95 eV. The detector was a parallel-plate photoelectron multiplier described elsewhere.[16] It was automatically moved along the Rowland circle and the spectra were recorded in the step-scanning mode. Because electron bombardment can decompose samples the electric power of the electron gun was kept low. When the first spectrum of a sample was taken only the main part of the spectrum between ~88 and 102 eV was measured within less than 10 min using a continuous recorder. After about 5 min from the beginning, the size of the focal spot (diameter 2–3 mm) became visible on the sample, but no further changes of the sample could be observed. These measurements were repeated and time was extended. Since the shape of the spectra did not change with time, we passed over to the step-scanning mode. The spectra were measured repeatedly, one run taking about 2–3 h. During the course of the measurements no changes of the spectra were observed. The spectra of several runs were identical, and therefore could be added up. A linear background was subtracted. The peak/background ratio varied from 19 (a-Si:H) to 4 (a-$SiO_{2.1}$:H).

In the figures the intensity (counts) is plotted vs photon

energy E. The $I(E)$-vs-E presentation is obtained from the original $I(x)$-vs-x data (x being the position of the exit slit on the Rowland circle) by using the identity $I(x)dx = I(\lambda)d\lambda = I(E)dE$.

3. O K emission bands

The O K emission bands were measured with our 11.5 m grazing incidence concave grating spectrometer (angle of incidence 87.8°).[17] A rotating Cu anode x-ray tube usually operated at 9100 V and 1.2 A was used for fluorescence excitation. The spectrometer is equipped with two turbomolecular pumps and a cryopump. The pressure in the spectrometer was 2×10^{-7} and 1×10^{-8} mbar in the x-ray tube, which is connected with the tank by a thin channel.

The holographic grating had 1200 lines/mm. The movement of the detector along the focal curve is accomplished by an x-y-locating arrangement controlled by a PC and operated in the step-scanning mode. The detector is a gas proportional counter (propane, 60 mbar).

8000–9000 counts were accumulated for the oxygen-rich samples ($x \geq 1.3$) and 5000–7000 for the oxygen-deficient samples. The peak/background ratio varied from 20 (a-$SiO_{2.1}$:H) to 4.3 (a-$SiO_{0.38}$). For evaluating the spectra the same procedure has been applied as for the Si L emission bands. The energy resolution of the spectrometer was about 0.6 eV at 526 eV.

III. EXPERIMENTAL RESULTS

In this section the Si K, Si L, and O K emission bands of a-SiO_x:H with $0 \leq x \leq 2.20$ are shown (Figs. 1–3, respectively) and the main features and their development with concentration x will be described.

A. Si K emission bands

Figure 1 shows the Si K emission bands for $x=0$ to $x=2.20$. In the concentration range $0 \leq x \leq 0.47$ the shape of the spectra develops gradually; the changes, however, are small. With increasing x the position of peak B is slightly shifted to lower photon energy, from 1836.25 for $x=0$ to 1836.05 eV (±0.05 eV) for $x=0.47$. The full width at half maximum (FWHM) is approximately constant (4.30±0.10 eV) for low concentrations and is slightly increased for $x=0.47$ (4.60 eV). Around 1832 eV there is a weak shoulder.

Going from $x=0.47$ to $x=0.83$ the spectrum changes considerably. The main peak B has broadened and shifted to lower photon energies (1835.5 eV) by 0.55 eV, thus leading to a less steep slope on the high-energy side. In the peak region some fine structure shows up. The shoulder at ~1832 eV has turned into a peak C whose intensity is about 80% of the main peak.

For $x=1.30$ the low-energy peak C has become the main maximum. With further increasing x it gets narrower; its position, however, remains at 1832.0 eV up to $x=2.20$. Parallel in the region 1834–1837 eV the relative intensity decreases and the fine structure (~1835 eV, ~1836 eV) disappears, resulting in a small peak at 1834.8 eV with about half the intensity of the maximum. For a-SiO_2 this intensity is only ~40%.

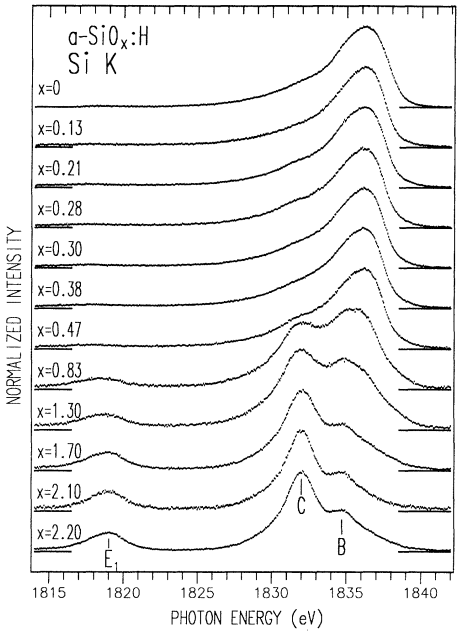

FIG. 1. Si K emission bands of a-Si:H ($x=0$) and of a-SiO_x:H ($0.13 \leq x \leq 2.20$).

The line-shaped feature E_1 around 1819 eV is very weak up to $x=0.47$. Between $x=0.47$ and $x=0.83$ its intensity increases remarkably. For higher x it further increases with increasing oxygen content of the samples. Simultaneously, its position moves to higher photon energy from about 1817.8 eV ($x \sim 0.4$) to about 1819.0 eV ($x \sim 2$).

B. Si L emission bands

The Si L emission bands of a-SiO_x:H with $0 \leq x \leq 2.20$ are shown in Fig. 2. The development of spectra with concentration x parallels that of the Si K emission bands.

The spectrum of amorphous hydrogenated silicon (a-Si:H) exhibits a broad peak (90.4 eV) and a shoulder on the high photon energy side. With increasing x the peak region develops some fine structure. The maximum becomes more pronounced and is slightly shifted to lower photon energies: from 90.4 eV for $x=0$ to 89.5 eV for $x=0.47$.

The spectra with $0 \leq x \leq 0.47$ are similar in shape. The spectrum for $x=0.83$, however, differs considerably (note that in the concentration range $x=0.47$ to $x=0.83$ also the Si L emission band has changed significantly): it exhibits two well-developed peaks D and B at 89.0 and 94.1 eV (intensity $I_D=100$, $I_B \approx 92$). The weak feature at 97.5 eV is residue of the pronounced shoulder at the high-energy edge for $x \leq 0.47$.

With further increasing concentration of oxygen the intensity of the saddle point I_{saddle} becomes lower and the two peaks become more pronounced. Compared to $x=0.47$ the intensity ratio I_D/I_B is approximately reversed and I_D/I_B decreases with increasing x. For $x=2.20$ the intensity ratio $I_D:I_{\text{saddle}}:I_B \approx 80:35:100$. The

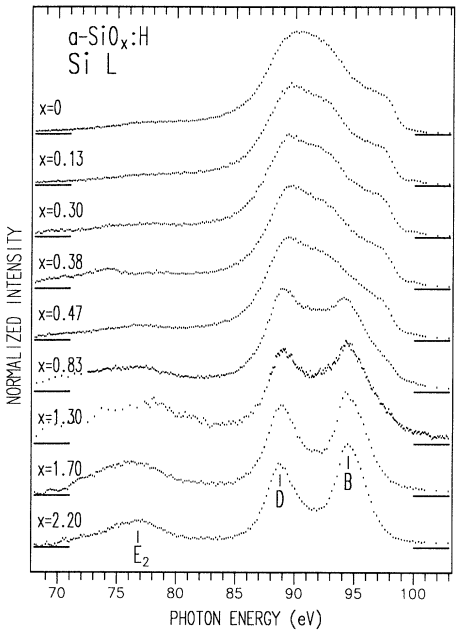

FIG. 2. Si L emission bands of a-Si:H ($x=0$) and of a-SiO_x:H ($0.13 \leq x \leq 2.20$).

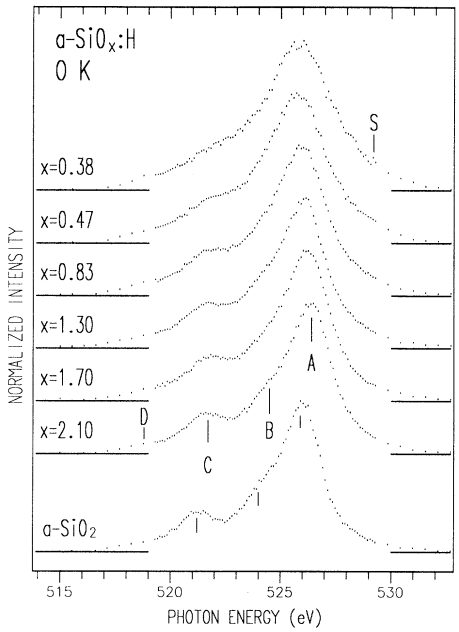

FIG. 3. O K emission bands of a-SiO_x:H ($0.38 \leq x \leq 2.10$) and of unhydrogenated a-SiO_2.

corresponding values for α-quartz are 75:37:100.

With increasing x the low-energy peak and the high-energy peak shift to lower and higher photon energy, respectively, thus leading to a larger energy separation of the two peaks. For $x=0.83$ the $D-B$ separation is 5.1 eV, for $x=2.2$ it is 5.9 eV.

The line-shaped feature E_2 at about 76–77 eV is superimposed in the low-energy part by other features which could not be identified and which also depend on sample composition. However, it can be clearly seen that the intensity of E_2 is very low up to $x=0.47$ and then rises quickly: for $x=0.83$ it is almost four times as intense as for $x=0.47$. For compositions with $1.3 \leq x \leq 2.2$ the intensity of E_2 is roughly constant. A similar behavior was also observed for E_1 (Fig. 1).

On the high-energy side of the Si L emission bands (99 to 101 eV) a weak shoulder is visible for concentrations up to $x=0.47$ which is absent at higher concentrations.

C. O K emission bands

Figure 3 shows the O K emission bands of a-SiO_x:H for selected oxygen concentrations x and for unhydrogenated a-SiO_2. The spectrum for $x=0.38$ is almost featureless with only two weak shoulders at ~ 522 eV (denoted by C) and at 518–519 eV (D). Maximum A is located at 525.75 eV (± 0.15 eV). With increasing oxygen concentration A is gradually shifted to 526.4 eV for $x=2.10$. The width of the spectrum (FWHM) narrows from 3.95 ± 0.05 eV ($x=0.38$) to 2.95 eV ($x=2.10$). Fine structure now becomes more clearly visible. Feature C shows a peak at 521.7 eV for concentrations with $1.3 \leq x \leq 2.1$. In this concentration range an additional weak feature shows up at ~ 524.5 eV (marked by B in Fig. 3).

As can be seen from Fig. 3 there is close similarity of the shape of the O K emission band of unhydrogenated a-SiO_2 to that with $x=2.10$; the spectrum of a-SiO_2, however, as a whole is shifted to lower photon energy by ~ 0.6 eV.

IV. DISCUSSION

As Figs. 1 and 2 show for concentrations $x \leq 0.47$ the shapes of the Si K and Si L emission bands do not differ significantly from that of a-Si:H. Although the concentration of oxygen in a-$SiO_{0.47}$ is considerable ($\sim 30\%$) the Si-Si bonds dominate and it seems that the silicon tetrahedrons are not disarranged by the presence of oxygen. The FWHM of the O K emission bands (Fig. 3) for $x=0.38$ and $x=0.47$ is larger than for $x=0.83$ and the spectra do not show any significant features, probably due to the different kinds of oxygen bonds with silicon.

Higher concentrations of oxygen distinctly reshape the Si K and Si L emission bands. At $x=0.83$ now features characteristic of SiO_2 show up: B, C, and D. Features characteristic of Si-Si bonds, however, are clearly observable up to concentrations $x=1.30$ at ~ 1836 eV (Si K) and ~ 97 eV (Si L).

The line-shaped peaks E_1 and E_2 originate from the corelike O $2s$ states. E_1 and E_2 are observable down to small concentrations x even though with very low intensity indicating the presence of Si-O bonds. As can be seen from Fig. 1 and—with some restrictions—also from Fig. 2, (i) the intensity of these O $2s$–derived states increases with increasing x and particularly between $x=0.47$ and $x=0.83$, and simultaneously (ii) their position shifts to higher photon energies. Both effects are a consequence of

the increasing number of Si-O bonds: an increasing oxygen content increases the intensity of the peaks formed by O 2*s* electrons and it also increases the charge transfer from silicon to oxygen atoms due to the high electronegativity of the oxygen atoms. This charge transfer shifts all silicon core levels towards higher binding energies and results in higher photon energy of E_1 and E_2 in the Si *K* and Si *L* emission bands, respectively. In fact, the shifts of the E_1 and E_2 peaks in x-ray photon energy scales provide the information which can distinguish between the two structural models suggested for the structure, based on the fourfold-bonded silicon and the twofold-bonded oxygen in the case of SiO_x alloys.

The first model is the random-bonding model (RBM), in which a statistical distribution of five basic bonding tetrahedral units, Si-Si_4, Si-Si_3O, Si-Si_2O_2, Si-SiO_3, and Si-O_4 is supposed. There are five possible bonding states for the Si atom in these units; the O atoms are each bonded to two Si atoms of different tetrahedra. The valence-electron charge transfer from Si to O creates a shift of silicon core levels. For the Si 2*p* level the shift is of about 1.05 eV per silicon-oxygen bond,[9] and for the Si 1*s* level we estimate the shift of about 1.20 eV per Si-O bond taking into account the energies of $K\alpha_1$ lines 1739.9 and 1740.5 eV in silicon and α-quartz (SiO_2) crystals, respectively.[18,19] Consequently, there are five different core-level positions of different Si atoms in RBM that correspond to five basic bonding units.

The second model is the random-mixture model (RMM). In the RMM of SiO_x the clusters of *a*-Si and SiO_2 are randomly dispersed and each has a domain size of a few tetrahedral units Si-Si_4 or Si-O_4. Contrary to the RBM, there are only two different core-level positions of different Si atoms separated by 4.2 eV. The other basic bonding units existing in RBM can be neglected in RMM due to only a small amount of these units at the boundary of a cluster.

The common structural feature of RBM and RMM is a twofold-bounded oxygen in SiO_x alloys. Supposing that oxygen atoms have the same local environment bridging in both models, the silicon tetrahedra, the oxygen core levels undergo no chemical shift dependent on oxygen concentration. The measured binding energy of the O 2*s* level in the SiO_x alloy in the concentration range $0.5 \leq x \leq 2.0$ is really stable and independent of x.[9]

Since x-ray emission spectra probe the local environment of the atom, the Si *K* and Si *L* emission bands of the SiO_x:H alloy are primarily determined by the nearest neighbors of Si in silicon tetrahedra while the arrangement of the tetrahedral basic bonding units in space has an effect on the details of the spectra.[18] This nearest-neighbor sensitivity has different consequences for spectra of RBM and RMM models.

In the case of RBM the binding energy of the core levels in different Si atoms will be different depending on how many oxygen atoms are present in basic bonding unit. As noted earlier the binding energy of O 2*s* is independent of concentration of oxygen. Consequently, the photon energy of the E_1 and E_2 peaks in XES of SiO_x alloys should depend on x. In the case of RMM, (i) the E_1 and E_2 peaks should have the same photon energy for all concentrations x since these peaks in XES come only from Si atoms surrounded always by four O atoms, and (ii) the XES of SiO_x should be very similar to the superposition of the spectra of *a*-Si and *a*-SiO_2 taking into account the Si, SiO_2 cluster composition of samples.

The superpositions of Si *K* emission bands of *a*-Si and *a*-SiO_2 corresponding in the SiO_x alloy to concentrations $x=0.47$, $x=0.83$, and $x=1.30$ are presented and compared with measured Si *K* bands of SiO_x:H in Fig. 4. The analogous superpositions of Si *L* emission bands are presented in Fig. 5. In the case of Si *K* bands in Fig. 4 we observe that the peak is shifted in the photon energy scale of about 0.4 and 0.7 eV for $x=1.30$ and $x=0.83$, respectively. This shift is related to the E_1 position in *a*-SiO_2. For $x=0.47$ the reliable position of E_1 cannot be determined. The observed shifts disprove the RMM model; however, the magnitudes of the shifts are too small to be in good agreement with the RBM. If we take into account the relative concentrations of the basic bonding units vs oxygen concentration x as shown by Bell and Ley in Fig. 2(a) of their work,[9] these shifts should be more or less two times larger than observed.

On the other hand, the remarkable agreement between the calculated superpositions in the valence-electron region at 1828–1840 eV and the measured Si *K* bands for $x=1.30$ and $x=0.83$ favors the RMM. In the case of $x=0.47$ the alloy spectrum is more similar to pure *a*-Si than to the corresponding mixture in Fig. 4. The same agreement between the calculated superpositions and the measurements can be seen for the valence-electron region of Si *L* bands at 86–99 eV presented in Fig. 5. Here the peak E_2 for the $x=1.30$ sample is practically not shifted contrary to the spectrum of the $x=0.83$ sample where the shift adequately corresponds to RBM. As mentioned

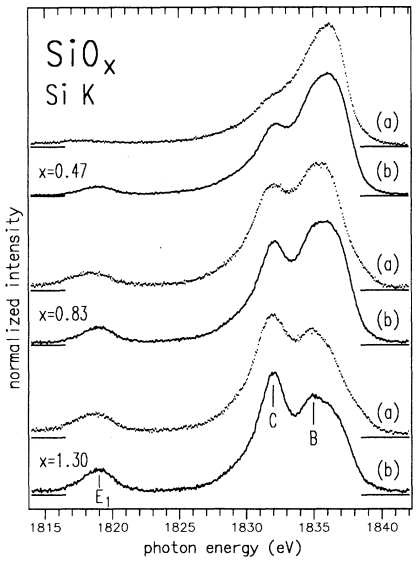

FIG. 4. Si *K* emission bands of *a*-SiO_x:H for intermediate oxygen contents: (a) measurement and (b) calculated superposition of measured bands of *a*-Si and *a*-SiO_2 with weighting factors corresponding to x.

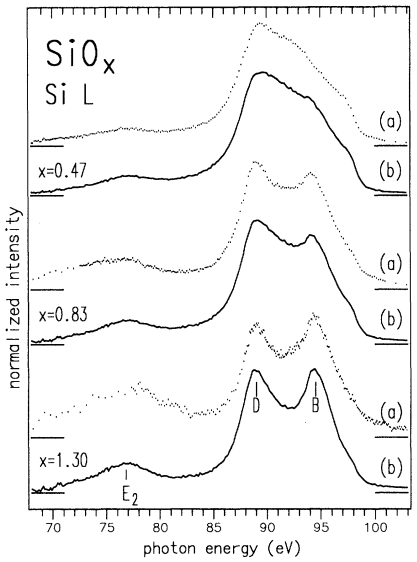

FIG. 5. Si L emission bands of a-SiO_x:H for intermediate oxygen contents: (a) measurement and (b) calculated superposition of measured bands of a-Si and a-SiO_2 with weighting factors corresponding to x.

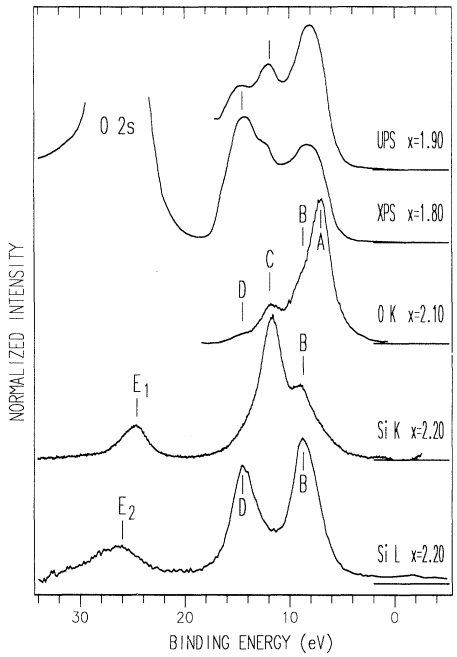

FIG. 6. X-ray emission bands (O K, Si K, Si L) and photoelectron valence-band spectra (Ref. 9) for high concentrations x ($1.90 \leq x \leq 2.20$) aligned on a common energy scale.

earlier, however, the feature E_2 is probably influenced by other factors.

As observed in Figs. 4 and 5, for some samples with intermediate concentration, the XES of SiO_x:H can be considered as superposition of XES of a-Si and a-SiO_2. It seems that the structure of some samples is closer to RMM and some of our samples are closer to RBM. Actually, the structure is more complex as has been discussed by Bell and Ley,[9] and it depends on the preparation conditions of samples.[20]

The comparison of XES with PES and theoretical results is very useful for the identification of the origin of observable valence-band features. In our Si K and Si L emission bands the photon energies are related to the Si $1s$ and Si $2p$ core levels, respectively, and we see in Figs. 1 and 2 the position of the valence electrons in the same energy intervals for all concentrations x. Also, the widths of the bands and the photon energies of the valence-band maxima remain nearly constant. Contrary to the XES in the PES the reference energy level is the Fermi energy, and therefore binding energies of Si core levels and the valence-band maxima depend on the composition of the samples. For that reason the direct comparison of the XES and PES measurements in a common energy scale can be carried out only in compounds having the same binding energies for relevant x-ray core levels.[21,22]

The Si K, Si L, and O K emission bands for high ($x = 2.10$) concentration are presented on a common binding energy scale in Fig. 6, together with UPS and/or XPS valence-band spectra of samples of similar composition. The UPS and/or XPS spectra and the corresponding binding energy scale were taken from the paper by Bell and Ley.[9] For the alignment of the x-ray emission bands with the UPS and/or XPS spectra we used the binding energies of the core levels[9] and the well-established character of the O $2s$ and Si $3s$ peaks, and the energies of the Si $K\alpha$ emission line. We estimate the accuracy of the mutual positions of the spectra in Fig. 6 to be about ± 0.2 eV.

The PES spectra presented in Fig. 6 were measured using samples which did not contain hydrogen. Actually, hydrogen does not affect the position of features of the UPS and/or XPS spectra on the binding energy scale,[9] and we also did not observe any effects caused by hydrogen comparing the Si K and Si L emission bands of a-SiO_2 and a-$SiO_{2.2}$:H samples. Therefore a direct comparison of these PES results with our silicon XES results seems to be justified. Hydrogen, however, affects the O K emission band. The O K emission band of a-$SiO_{2.2}$:H is shifted by 0.6 eV to higher photon energy compared to that of a-SiO_2 (Fig. 3). This shift originates from the higher binding energy of the O $1s$ level in hydrogenated a-$SiO_{2.2}$. The different binding energy of the O $1s$ level is probably caused by the replacement of some Si-O bonds by less ionic O-H and possibly O-O bonds. These changes reduce the negative charge on the oxygen atoms and give rise to an O $1s$ chemical shift.

The Si K, Si L, and O K emission bands for oxygen-rich samples ($x \sim 2$) are very similar to the corresponding spectra of α-quartz. It therefore is justified to discuss the experimental results in Fig. 6 on the basis of our calculations of the local partial densities of states (LPDOS) of α-quartz.

The computations are based on the self-consistent pseudopotential method. For the calculation of the LPDOS the wave functions calculated in the plane-wave basis set were projected into Gaussian s,p,d orbitals lo-

cated on the oxygen and silicon atoms. The values of α in the Gaussian factor $\exp(-\alpha r^2)$ are 1.5 and 1.0 for the oxygen and silicon atoms, respectively, to obtain projections which are sufficiently localized to avoid undesirable overlaps.

In Fig. 7 the total DOS and the LPDOS of α-quartz are shown. The lowest six bands at energies around 20 eV correspond to O $2s$-like electrons. The middle six valence bands in the energy range 5–10 eV constitute the O $2p$-, Si $3s$-, Si $3p$-, and Si $3d$-like bonding states. The upper 12 valence bands in the energy range 0–5 eV originate from a mixture of O $2p$-, Si $3s$-, Si $3p$-, and Si $3d$-like nonbonding states. These nonbonding states form the main peak of the UPS and O K spectrum. The electrons which occupy the 24 valence bands are localized mainly on the oxygen atoms. The spatial distribution of the above-mentioned three groups of valence bands was calculated by Allan and Teter.[5] The fact that the majority of the valence charge is localized on the oxygen atoms is accordingly reflected in the similarity of the oxygen LPDOS with the total DOS (Fig. 7).

Any variations of the valence-charge distribution induced by diverse Si-O bonds in the system a-SiO_x lead to larger relative changes of the small valence charge on silicon than on oxygen, and consequently also the LPDOS of silicon is being more affected than that of oxygen. This is the reason why the Si K and Si L emission bands to a large extent are sensitive to changes of concentration x while UPS and/or XPS and O K valence-band spectra preserve their main features almost throughout the concentration range x.

The short Si-O distance, the strong electronegativity of oxygen accompanied by charge redistribution, and the overlap of Si $3s$, Si $3p$, and originally empty Si $3d$ orbitals

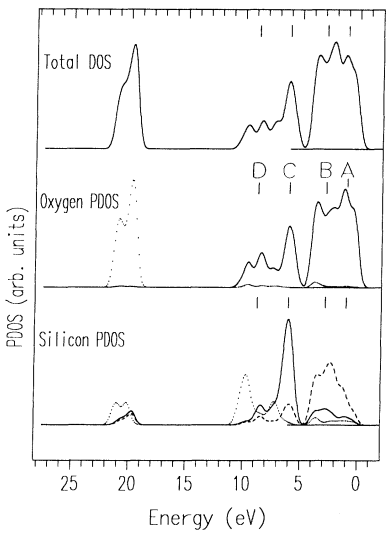

FIG. 7. Density-of-states curves of α-quartz (c-SiO_2). Top: total DOS; middle: oxygen partial DOS, (——) p-like DOS, (. . . .) s-like DOS; bottom: silicon partial DOS, (——) p-like, (. . . .) s-like, (— — —) d-like DOS. The zero of the energy scale relates to the top of the valence band. Notation and position of A, B, C, and D are taken from Fig. 6.

with O $2p$ electrons create a new atomic s,p,d configuration in both the Si and O atoms. Our calculations for α-quartz yield the following quantitative results for the s,p,d-like valence charge inside spheres around the oxygen ($r_O = 0.54$ Å) and silicon ($r_{Si} = 0.97$ Å) atoms.

Oxygen: total charge, 2.98; $2s^{1.22}$, $2p^{1.75}$.

Silicon: total charge, 1.98; $3s^{0.55}$, $3p^{0.90}$, $3d^{0.42}$.

In this example $r_O + r_{Si}$ is equal to the Si-O distance in α-quartz (1.51 Å) and r_O and r_{Si} are proportional to the radii of oxygen (0.66 Å) and silicon (1.17 Å) atoms in tetrahedral covalent bonds.[23] The s,p,d charge composition within these spheres of course depends on their radii: With increasing radius the amount of higher l components increases.

To estimate the effect caused by charge transfer or a new configuration of electrons the transition probabilities were calculated for several electron configurations and ionicities of the silicon atom. It was found that the ratio of the transition matrix elements $\langle 2p|r|3s\rangle / \langle 2p|r|3d\rangle$ is more sensitive to the ionicity of the silicon atom than to variations of the s,p,d electron configuration of the silicon atom. As a consequence the relative intensities of s-like and d-like peaks in the Si L emission bands ($3s \rightarrow 2p$ and $3d \rightarrow 2p$ electron transitions) yield experimental information about the ionicity of the silicon bond. Indeed the peaks of the Si L emission bands, as for instance of SiC,[24] Si_3N_4,[25,26] SiO,[27] SiO_2,[18,28] are in qualitative accordance with the electronegativity of the silicon partner.

The localization of most of the electrons on the oxygen site and the nonbonding character of the upper 12 valence bands are the key for resolving the so-called d-orbital controversy. For more than 20 years the question has been discussed of whether or not Si $3d$-like valence states participate significantly in the bonding of SiO_2.[13,22,29,30] There is quite a number of calculations based on oxygen $2s$ and $2p$ orbitals and silicon $3s$ and $3p$ orbitals which yield excellent agreement with photoemission data, the total energies, and the structural properties of SiO_2,[3,6] and therefore the inclusion of Si $3d$ orbitals in the basis set seemed to be superfluous. However, to our knowledge a conclusive explanation of the intensity distribution of the Si L emission band of SiO_2 (quartz), particularly of the origin of the main maximum B [see Fig. 6], is not available yet. Si L emission bands of various Si-O compounds were measured by several authors providing the same result: a characteristic double-peak spectrum.[18,19,27–29,31] The experimentalists argued that Si $3d$ states appear necessary to explain the spectral intensity in the upper part of the Si L valence-band spectra. On the other hand, quite recent first-principle calculations using a minimal set of only $2s2p$ and $3s3p$ orbitals per oxygen and silicon atom, respectively, result in equilibrium atomic geometries, charge distribution, force constants, and photoelectron spectra of amorphous SiO_x which are in good agreement with experimental results.[3] Therefore one might ask: Are the Si $3d$ states in SiO_2 redundant, and the Si L emission bands incorrectly interpreted?

Figure 8 shows the measured and calculated Si L emission band of α-quartz. The contribution of the s-like and d-like electrons were calculated separately and are included in the figure. The calculated Si L emission band exhib-

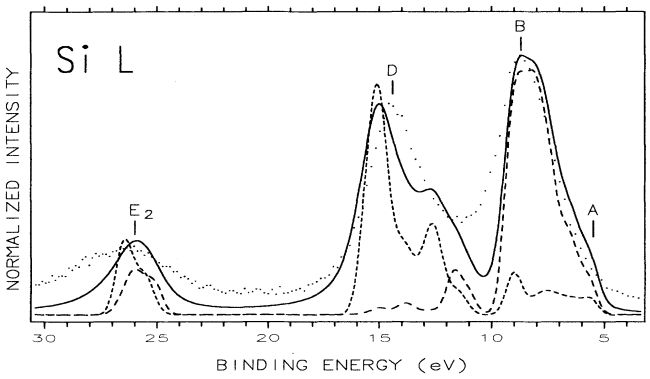

FIG. 8. Si L emission band of α-quartz (c-SiO_2): measured spectrum (points), calculated spectrum (full line), contribution of s-like electrons (short-dashed line), and contribution of d-like electrons (long-dashed line). The zero of the energy scale corresponds to that of Fig. 6.

its the same double-peaked shape as the measured spectrum. The positions of the peaks are identical in the measured and calculated spectra. The gap at about 10.5 eV and the shoulder at about 13 eV are smeared and not visible in the experiment. Details of the calculation will be published elsewhere.[32]

In view of our measurements of the Si L emission bands of various Si-O compounds and the good agreement between theory and experiment of all measured and calculated x-ray emission bands of α-quartz and stishovite,[32] we suggest the following interpretation which may resolve the long-standing d controversy.

The bonding states in Si-O compounds are governed by O $2s,2p$- and Si $3s,3p$-like electrons. These electrons form the lower 12 bands in α-quartz. The electrons forming the upper 12 bands in α-quartz are localized on the oxygen atoms and are of nonbonding character; for these electrons the description by O $2p$ orbitals is quite adequate as can be seen also from a contour plot of valence-charge densities of these states.[5] The structural properties are determined by bonds, i.e., by states having s,p character. PES measurements predominantly display O $2s,2p$ and Si $3s$ states. Therefore XPS and/or UPS spectra are appropriately described by the widely employed s,p basis calculations. XES, however, is a local probe and Si K and Si L emission bands delineate the Si $3p$ and Si $3s,3d$ character in a compound, respectively, i.e., they delineate the character of silicon located electrons. Since the total charge density on the silicon atoms is low only a small fraction of all the valence electrons makes a contribution to the silicon emission bands, and therefore even a small amount of Si d-like electrons clearly shows up in the Si L emission band. Accordingly, we conclude that Si K and Si L emission bands of Si-O compounds yield experimental data which provide a more stringent test for the electronic structure calculations than available UPS and/or XPS data.

V. SUMMARY

This work provides a comprehensive description of the local orbital character of the electrons in a-SiO_x: H alloy films based on Si K, Si L, and O K emission bands measured in the concentration range $0 \leq x \leq 2.2$. The development of features in the Si K and Si L emission bands runs parallel. The spectra, however, do not develop gradually; there is a strong reshaping of features between $x=0.47$ and 1.3. The pronounced changes of spectral features with x in both emission bands yield valuable information about the behavior of valence electrons in bonding and about basic bonding units Si-($Si_{4-n}O_n$), $n=0,1,\ldots,4$, of samples. The results to some extent favor the random-mixture model over the random-bond model. Our x-ray emission spectra unambiguously delineate the role of originally Si $3s,3p$ and O $2s,2p$ electrons in the bond and the formation of silicon d-like electrons due to silicon-oxygen interaction. The interpretation of the experimental results is supported by our *ab initio* calculation of the electronic structure of α-quartz. Since the local density of electrons is low in the vicinity of silicon atoms some properties (energy levels, total energy, or UPS and/or XPS spectra) are not significantly influenced by changes of the silicon sited orbital symmetry of valence electrons induced by the development of Si-O bonds in the system SiO_x:H. X-ray emission bands, however, and particularly the emission bands of electropositive elements are very sensitive to the relative changes of the LPDOS. Therefore XES supplies experimental data forming a stringent test of theoretical models.

ACKNOWLEDGMENTS

We thank Leibniz-Rechenzentrum der Bayerischen Akademie der Wissenschaften, München, for generously putting computer time at our disposal. A.Š. is greatly indebted to Deutsche Forschungsgemeinschaft for financial support.

[1]W. Y. Ching, Phys. Rev. B **26**, 6610 (1982); **26**, 6622 (1982); **26**, 6633 (1982).
[2]R. P. Gupta, Phys. Rev. B **32**, 8278 (1985).
[3]P. Ordejón and F. Ynduráin, Phys. Rev. B **43**, 4552 (1991), and references therein.
[4]J. R. Chelikowsky, H. E. King, Jr., N. Troullier, J. L. Martins, and J. Glinnemann, Phys. Rev. Lett. **65**, 3309 (1990).
[5]D. C. Allan and M. P. Teter, Phys. Rev. Lett. **59**, 1136 (1987).
[6]M. Hane, Y. Miyamoto, and A. Oshiyama, Phys. Rev. B **41**, 12 637 (1990).
[7]N. R. Keskar, N. Troullier, J. L. Martins, and J. R. Chelikowsky, Phys. Rev. B **44**, 4081 (1991).
[8]N. Binggeli, N. Troullier, J. L. Martins, and J. R. Chelikowsky, Phys. Rev. B **44**, 4771 (1991).
[9]F. G. Bell and L. Ley, Phys. Rev. B **37**, 8383 (1988).
[10]G. Wiech, W. Zahorowski, D. Baumüller, A. Šimůnek, and H. Watanabe, Phys. Scr. **41**, 1031 (1990).
[11]A. Šimůnek and G. Wiech, Solid State Commun. **76**, 955

(1990).
[12]J. J. Yeh and I. Lindau, At. Data Nucl. Data Tables **32**, 1 (1985).
[13]D. L. Griscom, J. Non-Cryst. Solids **24**, 155 (1977), and references therein.
[14]K. Haga and H. Watanabe, Jpn. J. Appl. Phys. **29**, 636 (1990).
[15]W. Zahorowski, J. Mitternacht, and G. Wiech, Meas. Sci. Technol. **2**, 602 (1991).
[16]W. Schnell and G. Wiech, Microchim. Acta, Suppl. **7**, 323 (1977).
[17]E. Gilberg, M. J. Hanus, and B. Foltz, Rev. Sci. Instrum. **52**, 662 (1981).
[18]G. Wiech and E. Z. Kurmaev, J. Phys. C **18**, 4393 (1985).
[19]E. Z. Kurmaev and G. Wiech, J. Non-Cryst. Solids **70**, 187 (1985).
[20]K. Hübner, Phys. Status Solidi **61**, 665 (1980).
[21]A. Šimůnek and G. Wiech, J. Non-Cryst. Solids **137&138**, 903 (1991).
[22]P. Ordejón, Solid State Commun. **83**, 175 (1992).
[23]Ch. Kittel, *Introduction to Solid State Physics* (Wiley, New York, 1976).
[24]W. Zahorowski, G. Wiech, H. Mell, and G. Weiser, J. Phys.: Condens. Matter **1**, 9571 (1989).
[25]G. Wiech, W. Zahorowski, A. Šimůnek, H. Mell, and G. Weiser, J. Non-Cryst. Solids **114**, 492 (1989).
[26]V. J. Nithianandam and S. E. Schnatterly, Phys. Rev. B **36**, 1159 (1987).
[27]T. Scimeca, Solid State Commun. **77**, 817 (1991).
[28]J. Nithianandam and S. E. Schnatterly, Phys. Rev. B **40**, 11 786 (1989).
[29]G. B. Cherlov, S. P. Freidman, E. Z. Kurmaev, G. Wiech, and V. A. Gubanov, J. Non-Cryst. Solids **94**, 276 (1987).
[30]E. Calabrese and W. B. Fowler, Phys. Rev. B **18**, 2888 (1978).
[31]G. Wiech, Solid State Commun. **52**, 807 (1984).
[32]J. Vackář, A. Šimůnek, and G. Wiech, J. Phys. Condens. Matter (to be published).